Energy & Environmental Science

ROYAL SOCIETY OF CHEMISTRY

PAPER

View Article Online
View Journal | View Issue

Cite this: *Energy Environ. Sci.*, 2021, **14**, 5523

Solvent-controlled O_2 diffusion enables air-tolerant solar hydrogen generation†

Michael G. Allan,[a] Morgan J. McKee,[a] Frank Marken[b] and Moritz F. Kuehnel *[ac]

Received 14th June 2021,
Accepted 20th August 2021

DOI: 10.1039/d1ee01822a

rsc.li/ees

Solar water splitting into H_2 and O_2 is a promising approach to provide renewable fuels. However, the presence of O_2 hampers H_2 generation and most photocatalysts show a major drop in activity in air without synthetic modification. Here, we demonstrate efficient H_2 evolution in air, simply enabled by controlling O_2 diffusion in the solvent. We show that in deep eutectic solvents (DESs), photocatalysts retain up to 97% of their H_2 evolution activity and quantum efficiency under aerobic conditions whereas in water, the same catalysts are almost entirely quenched. Solvent-induced O_2 tolerance is achieved by H_2 generation outcompeting O_2-induced quenching due to low O_2 diffusivities in DESs combined with low O_2 solubilities. Using this mechanism, we derive design rules and demonstrate that applying these rules to H_2 generation in water can enhance O_2 tolerance to >34%. The simplicity and generality of this approach paves the way for enhancing water splitting without adding complexity.

Broader context

Green hydrogen production is a key process for the transition to a carbon–neutral economy, but oxygen, ubiquitous in air and generated during water splitting, interferes with hydrogen generation. Not only does the presence of O_2 lower the hydrogen evolution efficiency, it can also degrade hydrogen evolution catalysts; in addition, O_2 causes problems in other key energy technologies, such as Li–O_2 batteries, fuel cells and in many other redox processes. The current approaches to improving O_2 tolerance add complexity and often come at the expense of consuming redox equivalents for O_2 removal, which lowers the overall efficiency. Here we show that by simply choosing solvents with a low O_2 diffusivity and solubility, photocatalysts normally inefficient for H_2 generation in air become highly O_2 tolerant, with minimal loss in activity and efficiency in air, even for extended periods of time. By unravelling the mechanism of the solvent-induced O_2 tolerance, we can translate it to achieve oxygen tolerance even in water, making it an important new concept with general applicability independent of the catalyst, solvent or process – a key step in making green H_2 production simpler and more efficient on a global scale.

Introduction

Solar hydrogen production from water is viewed as a viable method for generating clean renewable fuel to aid in combatting global energy challenges.[1,2] Materials employed for solar-driven H_2 production should be considered based on their cost, stability, toxicity and most importantly their practical applicability on a large scale. Real-world photocatalytic H_2 production systems must be active in the presence of O_2 generated *in situ* by water splitting and by exposure to air.[3] However, H_2 evolution in an aerobic environment is usually suppressed because of the more favourable oxygen reduction reaction.[4] In addition, molecular O_2 can inhibit H_2 evolution co-catalysts *via* interaction with the active site or by forming reactive oxygen species (ROSs).[5,6] Proton reduction in the presence of O_2 has been achieved by developing electrocatalysts with selectivity for H_2 evolution over O_2 reduction[7] or by creating a local anaerobic environment around the catalyst. Methods of lowering the effective O_2 concentration at the catalyst include O_2 reduction at catalysts capable of performing both O_2 reduction and H^+ evolution[8–10] and at organic dyes,[11] constructing layered architectures in which O_2 is reduced before it reaches the active site,[12–14] introducing antioxidant additives,[15,16] and modifying catalytic sites with O_2-blocking layers.[17–19] However, these approaches require a costly re-design of the catalyst to enhance O_2 tolerance and in many cases photons and charges are used to reduce O_2, leading to a decrease in quantum and faradaic yield, respectively. Recent work has demonstrated O_2-tolerant CO_2 reduction enabled by controlling O_2 diffusion to the electrode using selective membranes and coatings.[20,21] Related approaches have been used in lithium–oxygen batteries.[22]

[a] *Department of Chemistry, Swansea University, Singleton Park, Swansea SA2 8PP, Wales, UK. E-mail: m.f.kuehnel@swansea.ac.uk*
[b] *Department of Chemistry, University of Bath, Claverton Down, Bath BA2 7AY, UK*
[c] *Fraunhofer Institute for Microstructure of Materials and Systems IMWS, Walter-Hülse-Straße 1, 06120 Halle, Germany*

† Electronic supplementary information (ESI) available: Experimental details, additional tables and figures. See DOI: 10.1039/d1ee01822a

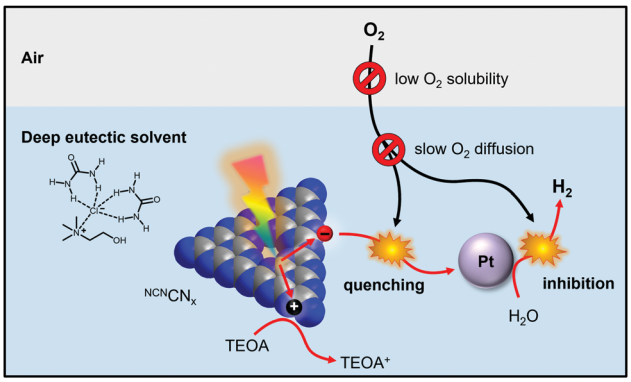

Fig. 1 Schematic representation of solvent-mediated oxygen-tolerant photocatalytic hydrogen production in deep eutectic solvents demonstrated in this work.

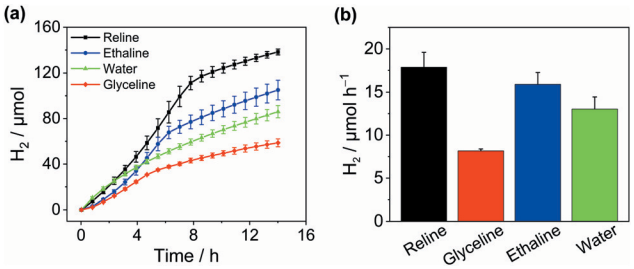

Fig. 2 Photocatalytic H_2 generation in DESs at Pt/$^{NCN}CN_x$: (a) H_2 production in different DESs and water; (b) max. H_2 production rate in DESs *vs.* H_2O. Conditions: $^{NCN}CN_x$ (2.0 mg), H_2PtCl_6 (0.05 mg Pt), in 2.0 mL DES (12.5% v/v H_2O, 0.38 M TEOA, 2 mM MV^{2+}) or water (0.38 M TEOA, pH 7, no MV^{2+}); AM 1.5G, 1 sun, 40 °C, constant N_2 purge.

To date, research in hydrogen evolution has not exploited solvent effects for promoting O_2 tolerance, even though O_2 solubility and diffusivity in the reaction medium are the primary factors controlling the availability of O_2 to the catalytically active site.

In this work we demonstrate that using deep eutectic solvents (DESs) as a reaction medium enables O_2-tolerant photocatalytic H_2 production with O_2-intolerant photocatalysts without making any catalyst modifications and without affecting the quantum efficiency. DESs are an alternative class of low-cost, highly tuneable ionic liquids[23] that can be prepared from readily available precursors and possess lower toxicities than conventional ionic liquids.[24] DESs have been employed for air-tolerant organic reactions involving highly reactive organolithium compounds[25,26] and it has recently been shown they can stabilise O_2-sensitive radicals in air.[27] Using a carbon nitride photocatalyst, we now show that DESs create a near-anaerobic environment in which up to 97% of the photocatalytic H_2 evolution activity is retained under air (Fig. 1). Mechanistic studies reveal a close interplay between O_2 solubility and diffusivity and allow us to develop a quantitative model of the O_2 tolerance. Based on this model we derive key design criteria for tailored reaction media that promote efficient and cost-effective O_2 tolerance with established H_2 generation photocatalysts without synthetic modification.

Results and discussion

Deep eutectic solvents as a medium for solar H_2 generation

To investigate solvent effects on the photocatalytic H_2 evolution performance, we chose cyanamide-functionalised carbon nitride ($^{NCN}CN_x$) as a model photocatalyst (Fig. S1–S4, ESI†)[28,29] and studied its activity in three well-known type-III DESs, namely choline chloride–urea 1:2, choline chloride–glycerol 1:2, and choline chloride–ethylene glycol 1:2, termed reline, glyceline and ethaline, respectively. These solvents were chosen due to their facile preparation, low cost, low toxicity and infinite miscibility with water.[23] Pt was used as a HER co-catalyst, *in situ* photodeposited from H_2PtCl_6 (Pt/$^{NCN}CN_x$). In reline, Pt/$^{NCN}CN_x$ generated 138.3 ± 2.6 μmol_{H_2} after 14 h irradiation with simulated solar light (AM 1.5G, 1 sun) at an activity of 8.9 ± 0.9 $mmol_{H_2}$ $g_{CN_x}^{-1}$ h^{-1} using triethanolamine (TEOA) as a sacrificial electron donor (Fig. 2). Addition of water (12.5% by volume) was essential as in neat DESs, H_2 evolution activity was negligible (Fig. S5, ESI†). The same conditions yielded an activity of 8.0 ± 0.6 and 4.1 ± 0.1 $mmol_{H_2}$ $g_{CN_x}^{-1}$ h^{-1} for ethaline and glyceline, respectively with cumulative values of 105.1 ± 8.6 and 58.7 ± 3.5 μmol_{H_2} after 14 hours (Table S1, ESI†). Depending on the solvent, a decay in activity was observed after 5–9 h which we attribute to the well-known decomposition of the redox mediator methyl viologen (MV^{2+})[30] as with a further addition of MV^{2+}, the rate increased again (Fig. S6, ESI†). In the absence of MV^{2+}, H_2 evolution was slower but no decay in activity was observed (Fig. S7, ESI†) proving that the DESs do not compromise the stability of the $^{NCN}CN_x$ photocatalyst. In water, $^{NCN}CN_x$ displayed a maximum activity of 6.5 ± 0.7 $mmol_{H_2}$ $g_{CN_x}^{-1}$ h^{-1} and a cumulative production of 86.1 ± 5.4 μmol_{H_2} after 14 h irradiation under optimised conditions (0.38 M TEOA, pH 7.0, no MV^{2+}) which is on par with recent literature values.[29] This was lower in comparison to reline and ethaline and higher than the activity in glyceline (see Fig. S8 and S9, ESI† for optimisation and controls). The external quantum efficiency for H_2 evolution in reline was determined at 3.7 ± 1.5% and was stable even after 20 h of irradiation (Table S2, ESI†). We can therefore state that under the given conditions, DESs are a competitive solvent with water for solar H_2 generation.

A notable difference between water and DES is the effect of added MV^{2+} on the H_2 evolution: While adding MV^{2+} increases H_2 generation in DES, a decrease in activity is observed in water (Fig. S10, ESI†). A suppression of H_2 evolution upon addition of the redox mediator MV^{2+} has been previously observed in cases where there is good electron transfer between the photocatalyst and the HER co-catalyst.[31] In this case, adding MV^{2+} does not enhance HER but instead causes a visible accumulation of reduced $MV^{+\bullet}$ in the solution which blocks light penetration to the photocatalyst due to its deep blue colour. The beneficial effects of adding MV^{2+} in DESs, in turn, suggest poor electron transfer between $^{NCN}CN_x$ and Pt in DESs. To prove this, we performed recycling experiments in which we separated the photocatalyst after 4 h irradiation in the presence of H_2PtCl_6

from its supernatant and re-suspended it in a fresh solution without added Pt, before continuing irradiation. In water, the photocatalytic H_2 evolution activity was not affected by this procedure, suggesting Pt is deposited on the $^{NCN}CN_x$ photocatalyst (Fig S11, ESI†), in line with previous literature. In DES, however, the photocatalytic activity was almost completely quenched, corroborating poor immobilisation of Pt on $^{NCN}CN_x$ in DES, possibly due to differences in solvation in DESs.

O_2-tolerant H_2 generation in DESs

Inspired by their application as solvents to perform air-sensitive syntheses under an aerobic atmosphere,[25,26] we set out to achieve air-tolerant H_2 evolution in DESs. It is well known that photocatalytic H_2 evolution is suppressed in air even for highly active materials[32] arising from the thermodynamically favourable O_2 reduction and quenching of the photosensitiser. Fig. 3a indicates that Pt/$^{NCN}CN_x$ generates only 0.8 ± 0.2 $mmol_{H_2}$ $g_{CN_x}^{-1}$ h^{-1} upon irradiation in aerated water corresponding to a retention of only $8.8 \pm 1.5\%$ of its photocatalytic activity seen under inert conditions. When the redox mediator MV^{2+} was added the retention dropped to $1.7 \pm 0.7\%$. However, in the DES reline, the same catalyst without any modification achieved an activity of up to 8.7 ± 0.9 $mmol_{H_2}$ $g_{CN_x}^{-1}$ h^{-1} in air, corresponding to a remarkable activity retention of up to $97.3 \pm 17.5\%$ compared to anaerobic conditions (Fig. 3b and Table S3, ESI†). While the O_2 tolerance in water decreases further over time with almost complete deactivation after 10 h, DESs maintain a high level of O_2 tolerance over prolonged periods of time (Fig. S12, ESI†). After 14 h, 123.5 ± 8.1 μmol_{H_2} were produced in air (Fig. 3c) corresponding to $89.3 \pm 6.1\%$ of the amount produced under N_2 and the system remained active (Fig. 3d). Similarly, an activity of 5.7 ± 1.3 $mmol_{H_2}$ $g_{CN_x}^{-1}$ h^{-1} was seen in aerobic ethaline ($73.5 \pm 9.0\%$ retention) and 3.6 ± 0.3 $mmol_{H_2}$ $g_{CN_x}^{-1}$ h^{-1} in aerobic glyceline ($90.4 \pm 7.9\%$ retention). The external quantum efficiency for H_2 evolution in aerobic reline was determined at $3.9 \pm 0.3\%$ after 20 h of irradiation (Table S4, ESI†) which is within error identical to the EQE observed in anaerobic conditions. The optimum O_2 tolerance was observed at 12.5% water content. Increasing the water content led to a lower O_2 tolerance (Fig. S13, ESI†), whereas without added water, H_2 evolution activity was much lower, presumably for lack of available protons (Fig. S5, ESI†).

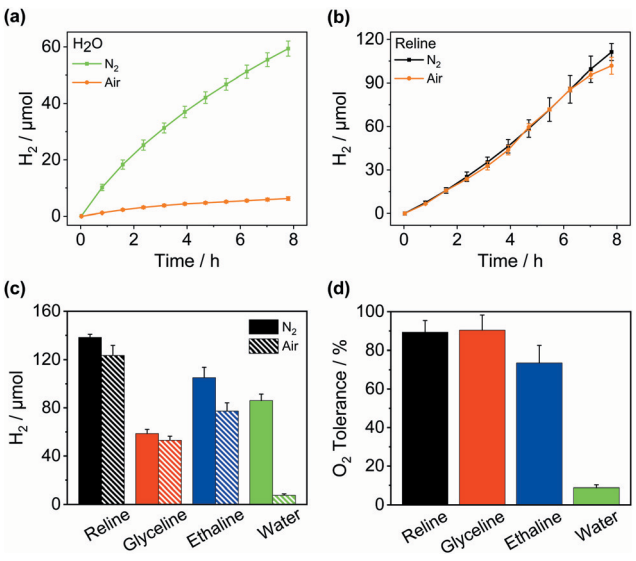

Fig. 3 Solvent-mediated oxygen-tolerant H_2 generation at Pt/$^{NCN}CN_x$. Effect of aerobic conditions on H_2 production in (a) H_2O and (b) reline; (c) total H_2 evolved after 14.0 h under anaerobic and aerobic conditions in different DESs and H_2O; (d) relative H_2 evolution activities under aerobic conditions depending on the solvent. Conditions: $^{NCN}CN_x$ (2.0 mg) H_2PtCl_6 (0.05 mg Pt) in 2.0 mL DES (12.5% v/v H_2O, 0.38 M TEOA, 2 mM MV^{2+}) or water (0.38 M TEOA, pH 7); AM 1.5G, 1 sun, 40 °C, constant air purge.

The O_2 tolerance induced by DESs compares favourably with examples of O_2-tolerant H_2 evolution from the literature (Table S5, ESI†). A range of CdS-based photocatalysts[33–35] achieve O_2 tolerances between 40–80%; air can even increase the activity of CdS by suppressing photocorrosion.[36] These studies typically operate at high H_2 production rates due to high electron donor concentrations, closed photoreactors and often high light intensities, where O_2 in the solution and the reactor headspace is rapidly depleted by reduction to H_2O, effectively generating anaerobic conditions *in situ.* This is often indicated by an observed lag period before H_2 evolution occurs. In contrast, H_2 production in DESs shows no detectable lag period and a high O_2 tolerance despite a continuous air purge maintaining a constant O_2 concentration. The latter is particularly important to exploit O_2 tolerance to enhance overall water splitting, where O_2 is continuously generated and H_2 production rates are much lower than in sacrificial systems. Photocatalysts operating at lower rates where O_2 depletion is less effective have shown lower O_2 tolerances, *e.g.* RuP/CoP/TiO_2 (17% O_2 tolerance),[9] Ni_2P/OH-GQD (64%)[37] and PFBT polymer dots (37%).[38] To the best of our knowledge, there is no literature on O_2-tolerant H_2 generation using carbon nitride-based photocatalysts.

The advantage of solvent-induced O_2 tolerance lies in its applicability independent of the photocatalyst. When Pt/TiO_2 was used as the photocatalyst instead of Pt/$^{NCN}CN_x$, the O_2 tolerance similarly increased from $29.6 \pm 6.5\%$ in water to $86.1 \pm 12.8\%$ in reline after 12 h irradiation (Fig. S14, ESI†), proving this effect is not limited to a single photocatalyst. To further demonstrate the generality of this approach, we also studied H_2 evolution at the homogeneous photocatalyst Pt/Eosin Y (Pt/EY).[39] Even though the H_2 evolution in ethaline and reline (17.5 ± 1.7 μmol_{H_2} $mmol_{EY}^{-1}$ and 11.4 ± 1.7 $mmol_{H_2}$ mol_{EY}^{-1} after 5.5 h, respectively, non-optimised conditions, Fig. S15, ESI†) was slower than in water (81.1 ± 6.8 μmol_{H_2} $mmol_{EY}^{-1}$), the DESs promote excellent retention of activity in air. Pt/EY in aerobic H_2O produced 0.7 $mmol_{H_2}$ mol_{EY}^{-1} after 5.5 h (<1% activity retained), whereas 14.9 $mmol_{H_2}$ mol_{EY}^{-1} was generated in ethaline corresponding to 85.5% O_2 tolerance. This, again, compares well with literature examples of aerobic H_2 evolution at homogeneous photocatalysts,[40–42] *e.g.* CoP/EY retained $70 \pm 4\%$ activity in air, however activity was limited to 2 h.[9]

The mechanism of solvent-induced O_2 tolerance

Having demonstrated that DESs promote O_2 tolerance of photocatalytic H_2 evolution independent of the photocatalyst, we sought to gain understanding of the underlying mechanism. Previous work on DESs enabling air-tolerant alkylation with organolithium and Grignard reagents suggested that the high halide concentration in DESs increases the reagents' reactivity to levels where they can outcompete hydrolysis. However, no explanation for the observed insensitivity to O_2 was given.[25,43] To elucidate the mechanism by which DESs promote O_2-tolerant H_2 evolution, we first studied the formation and stability of reduced $^{NCN}CN_x$ in both H_2O and DESs in air. $^{NCN}CN_x$ is known to form a turquoise-blue photoreduced state $^{NCN}CN_x^*$ originating from charge accumulation in the material when irradiated in the presence of an electron donor and absence of a hydrogen evolution co-catalyst.[29] $^{NCN}CN_x^*$ persists in an anaerobic environment but is quenched rapidly by reaction with O_2. In water, $^{NCN}CN_x^*$ is therefore only formed under N_2 and immediately quenched upon exposure to air as indicated by the blue material regaining its original yellow colour. However, when $^{NCN}CN_x$ is irradiated in DESs, $^{NCN}CN_x^*$ is quickly formed even in an aerated solution. Moreover, the blue colour is stable in air for several days, with a noticeable absorbance at ~680 nm in the DR-UV spectrum, ascribed to the reduced photocatalyst (Fig. 4). This absorbance is not observed in an aerated aqueous solution, highlighting the solvent effect on limiting the quenching of the photoabsorber by reaction with O_2. To further corroborate the absence of O_2 quenching in aerated DESs, we investigated photocatalytic degradation of the organic dye methylene blue in aerated DESs using $^{NCN}CN_x$ as a photocatalyst. Dye degradation relies on reactive oxygen species (ROSs) such as O_2^- to act as oxidants, generated by the quenching of the excited state of a photocatalyst by O_2; it is therefore strongly dependant on dissolved O_2.[44] Consistently, we observed that the degradation of methylene blue was much slower in DESs than in water, which lends further evidence to a suppression of O_2 quenching depending on the solvent (Fig. S16, ESI†).

Further quantitative insight was sought from determining the saturation concentration and diffusion coefficient of O_2 in DESs by studying the electrochemical O_2 reduction at a Pt microwire electrode.[45] Potential step chronoamperometry was performed in each solvent and the observed current transients for the electrocatalytic O_2 reduction were fitted according to the Shoup–Szabo equation[46] to simultaneously derive the O_2 concentrations and the O_2 diffusion coefficients in aerated DESs and water, under the conditions tested for photocatalytic H_2 evolution (Table 1 and Fig. S17–S20, ESI†).[47] All the DES-based solutions exhibited lower O_2 solubilities than conventional organic solvents,[48,49] presumably due to their high ionic strengths causing a salting-out effect.[50,51] In addition, O_2 diffusion coefficients were found to be lower than in most other solvents[48,49] including water[52] but varied strongly between the different DESs. This behaviour is likely a result of their high viscosities combined with their complex liquid structure,[53] in which hydrogen bond donor dependent cluster formation presumably influences molecular diffusion in the liquid as well as causing large variations in viscosity.[54]

Table 1 O_2 solubility and diffusivity in different solvents determined by microwire chronoamperometry and observed O_2 tolerance during photocatalytic H_2 generation in these solvents. Conditions: DES (12.5% H_2O, 0.38 M TEOA, 2 mM MV) or water (0.38 M TEOA, pH 7), 40 °C; photocatalysis: $^{NCN}CN_x$ (2.0 mg), H_2PtCl_6 (0.05 mg Pt) in 2.0 mL solvent, (AM 1.5G, 1 sun, constant air purge)

Solvent	$c(O_2)$ [μM]	$D(O_2)$ [$m^2\ s^{-1}$]	O_2 tolerance[a] [%]
Reline	167.8 ± 9.1	2.93 ± 0.02 × 10^{-10}	89.3 ± 6.1
Ethaline	250.7 ± 0.4	3.32 ± 0.01 × 10^{-10}	73.5 ± 9.0
Glyceline	218.8 ± 2.0	9.52 ± 0.01 × 10^{-11}	90.4 ± 7.9
H_2O	223.5 ± 0.4	2.94 ± 0.01 × 10^{-9}	8.8 ± 1.5[b]

[a] O_2 tolerance = total H_2 produced under air relative to total H_2 produced under N_2 at Pt/$^{NCN}CN_x$ after 14 h irradiation under otherwise identical conditions. [b] Without added MV^{2+}.

We expect O_2 tolerance to be a function of the effective O_2 concentration at the photocatalyst surface, which depends on both solubility and diffusivity of O_2 in the reaction medium. Comparing the trends in these parameters for the different DES-based solutions to the trend in O_2 tolerance shows a clear correlation between the observed retention of photocatalytic activity in air (glyceline ≈ reline > ethaline > water) and the O_2 diffusivities (glyceline < reline < ethaline < water). As O_2 in solution is being consumed due to O_2 reduction at the photocatalyst, the steady-state O_2 concentration at the catalyst surface depends on how rapidly more O_2 is supplied to the photocatalyst, therefore O_2 tolerance is primarily dominated by the O_2 diffusivity. The O_2 solubility of the solutions (reline < glyceline < ethaline < water) is of secondary importance: glyceline and reline solutions show comparable O_2 tolerances despite them showing varying O_2 solubilities and diffusivities – this is likely because the lower diffusivity in glyceline is compensated by a higher O_2 solubility, and *vice versa*. Water shows poor O_2 tolerance because it exhibits the highest O_2 diffusion coefficient among the solvents studied here and a relatively high O_2 solubility. Due to a combination of low O_2 diffusivities and low O_2 solubilities, DESs thus create pseudo-inert conditions by limiting O_2 mass transport, which is outcompeted by H^+ diffusion.

Having identified the combination of low O_2 solubility and O_2 diffusivity as key factors to O_2 tolerance, we use these design

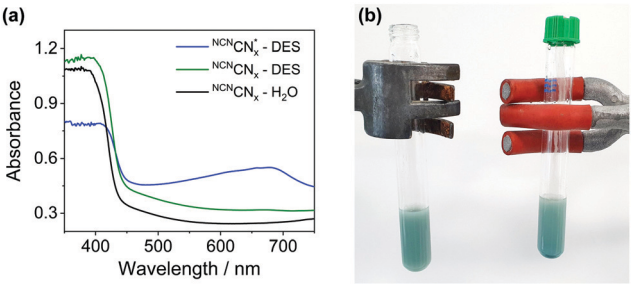

Fig. 4 (a) Absorption spectra of $^{NCN}CN_x$ in DES TEOA solution (green trace) and aqueous TEOA solution (black trace) prior to irradiation with simulated solar light. $^{NCN}CN_x^*$ absorption spectra in DES TEOA solution (blue) recorded in ambient air. (b) Photo of $^{NCN}CN_x^*$ in DES solutions exposed to air (left) and in inert atmosphere (right).

Table 2 O_2 solubility and diffusivity in brines of different concentration and observed O_2 tolerance during photocatalytic H_2 generation. Conditions: $^{NCN}CN_x$ (2.0 mg), H_2PtCl_6 (0.05 mg Pt) in 2.0 mL water (0.38 M TEOA, pH 7, 2 mM MV^{2+}); (AM 1.5G, 1 sun, 40 °C, constant air purge)

Solvent[a]	$c(O_2)$ [μM]	$D(O_2)$ [$m^2\ s^{-1}$]	O_2 tolerance[b] [%]
0 M NaCl	223 ± 0.4	$2.94 \pm 0.01 \times 10^{-9}$	3.1 ± 1.7
1 M NaCl	265 ± 0.6	$2.30 \pm 0.01 \times 10^{-9}$	13.9 ± 3.3
2 M NaCl	165 ± 0.2	$1.55 \pm 0.01 \times 10^{-9}$	19.0 ± 11.4
4 M NaCl	128 ± 0.3	$1.13 \pm 0.01 \times 10^{-9}$	34.2 ± 4.4

[a] Solubilities were determined under the same conditions as the photocatalysis experiments were performed. [b] O_2 tolerance = total H_2 produced under air relative to total H_2 produced under N_2 at $Pt/^{NCN}CN_x$ after 14 h irradiation under otherwise identical conditions.

criteria to promote O_2 tolerance in other solvents. Saline water is an attractive feedstock for renewable H_2 production since seawater is much more abundant than freshwater and its use avoids competition with drinking water supplies.[55] While using seawater can be challenging, we show here that it can enable highly O_2-tolerant H_2 evolution. It is well known that high salt concentrations lower the O_2 solubility in water as well as the O_2 diffusion coefficients.[47,56] We therefore determined the O_2 solubility and diffusivity in brines under photocatalysis conditions (40 °C, 0.38 M TEOA, pH 7) by microwire electrochemistry. Table 2 shows that the O_2 solubility and diffusivity both decrease by approx. 50% upon increasing the NaCl concentration from 0 to 4 M. Consistently, Fig. 5 demonstrates that in line with our identified design criteria, the O_2 tolerance in water increases with increasing NaCl concentrations. In 4 M aqueous NaCl a cumulative O_2 tolerance of 34.2 ± 4.4% is observed after 14 h (Fig. S21 and Table S6, ESI†), more than 10 times higher than without added NaCl (Table 2). However, despite lower O_2 solubilities, the O_2 tolerance never reaches the levels observed in DESs consistent with the higher O_2 diffusion coefficient in water. This demonstrates that the O_2 diffusivity is decisive for the overall O_2 tolerance, ideally when paired with a low O_2 solubility. Furthermore, we studied the direct use of seawater collected from Swansea Beach as a solvent for H_2 evolution (Fig. S22, ESI†). While the H_2 generation activity was lower than in pure brines, presumably due to its brownish colour, the observed O_2 tolerance of 7.2 ± 4.4% was higher than in pure DI water. Considering the local salinity of 0.41–0.53 M,[57] this data is in good agreement with Table 2 and demonstrates the usefulness of using non-potable water for solar H_2 generation.

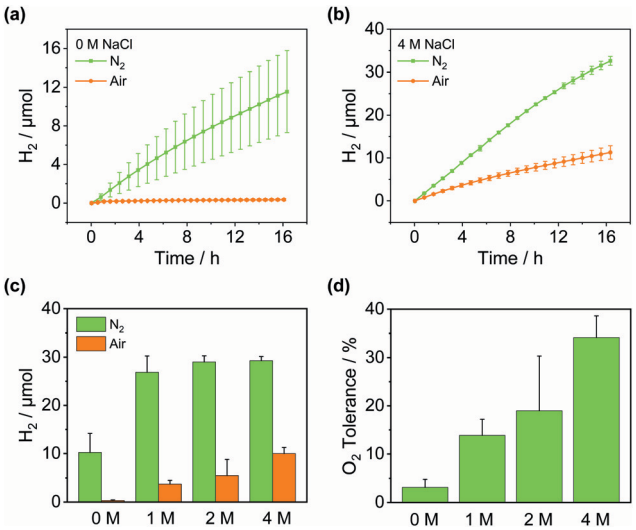

Fig. 5 Enhanced oxygen tolerance by control of O_2 diffusion. Effect of aerobic conditions on H_2 production in (a) H_2O and (b) 4 M aqueous NaCl; (c) total H_2 evolved after 14.0 h depending on the NaCl concentration and atmosphere; (d) O_2 tolerance of H_2 evolution depending on the NaCl concentration. Conditions: $^{NCN}CN_x$ (2.0 mg) H_2PtCl_6 (0.05 mg Pt) in 2.0 mL saline water (0.38 M TEOA, pH 7, 2 mM MV^{2+}); AM 1.5G, 1 sun, 40 °C, constant N_2 or air purge.

Design rules from a quantitative model for O_2 tolerance

To explain the effect of O_2 diffusivity and solubility on the O_2 tolerance quantitatively, we have developed a mechanistic model based on fluxes to and from the photocatalyst particles (Fig. 6a). The rate of charge carrier generation, $R(h\nu)$, depends on light intensity and quantum efficiency and is assumed largely independent of the solvent. O_2 is expected to quench charge carriers with consuming O_2, expressed as the rate $R(O_2)$. Approximating the O_2-dependent quenching as O_2 reduction at a spherical particle at the limit of diffusional control gives eqn (1):

$$R(O_2) = 4\pi \times r \times n \times D(O_2) \times c(O_2) \quad (1)$$

with r the particle radius and n the number of electrons quenched per O_2 molecule.[47] The flux of H_2 from the particle, $R(H_2)$, is assumed not impeded. The O_2 tolerance can then be expressed as the efficiency of H_2 production in competition with O_2-dependent quenching (eqn (2)), which upon expressing $R(O_2)$ according to eqn (1) shows a linear dependence of the O_2 tolerance on the product of $D(O_2)$ and $c(O_2)$ (eqn (3)):

$$O_2\ \text{tolerance} = 100\% \times \frac{R(H_2)}{R(h\nu)} = 100\% \times \frac{R(h\nu) - R(O_2)}{R(h\nu)} \quad (2)$$

$$O_2\ \text{tolerance} = \left(1 - \frac{4\pi rn}{R(h\nu)} \times D(O_2) \times c(O)_2\right) \quad (3)$$

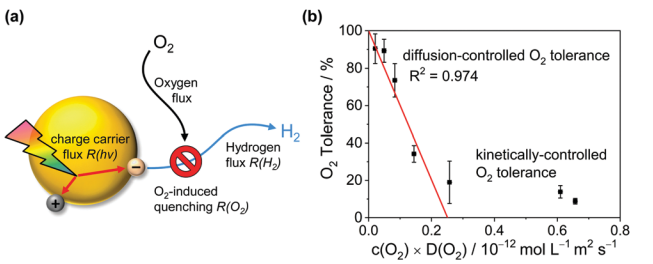

Fig. 6 Mechanistic model for the solvent-induced O_2 tolerance. (a) Schematic illustration of fluxes to and from the photocatalyst particle. (b) Plot of the O_2 tolerance for H_2 evolution *versus* the product of $D(O_2)$ and $c(O_2)$ in the respective reaction medium fitted according to eqn (3).

Fig. 6 shows that the experimentally observed O_2 tolerances fit well to this model (see ESI† for details). At high O_2 tolerances, the slope represents the consumption of photo-generated charge carriers by O_2 in diffusion-limited quenching. When the O_2 flux increases with higher O_2 solubility and diffusivity, the quenching process is no longer diffusion limited but instead kinetically limited by the rate of O_2 reduction, resulting in O_2 tolerance gradually tailing towards zero at a much lower slope. From this model, we can infer a set of design rules for improving O_2 tolerance through further solvent design:

1. Minimise the $c \times D$ parameter (low O_2 solubility and diffusivity, high viscosity).
2. Decrease particle size (large particles increase O_2 flux).
3. Increase light intensity (outcompete O_2 flux which is independent of light).
4. Increase photon-to-charge carrier conversion.

Future work should focus on exploring all variables of the model to further verify and refine its predictive ability and achieve sustained, fully O_2-tolerant H_2 generation.

Conclusions

We have shown that O_2-tolerant H_2 evolution can be achieved by controlling O_2 diffusion and solubility in the reaction medium. We introduced DESs as a versatile medium for solar H_2 generation with both heterogenous and homogenous light absorbers and showed that DESs induce a high O_2 tolerance to otherwise O_2-intolerant photocatalysts without compromising the quantum efficiency. We demonstrated this effect results from their low O_2 solubilities and diffusivities. Exploiting these properties as design criteria enables a 10-fold increase in O_2 tolerance in water by controlling O_2 diffusion and solubility. Through developing a quantitative model for oxygen tolerance, we believe this investigation paves the way for further solvent-enhanced solar fuel production and, owing to the tuneable nature of DESs, allows for a wide scope of solvents to be examined. The fact that a relatively small change in the solvent constituents (replacing ethylene glycol with glycerol) causes a considerable change in the O_2 diffusivity and thus in the O_2 tolerance demonstrates the enormous potential of solvent design for solar water splitting, yet it highlights the need for establishing structure–function relationships to allow a rational solvent design. Future studies will expand the concept of O_2 diffusion control to fully explore all parameters of our model with the potential to massively enhance solar water splitting without adding complexity.

Data availability

Raw experimental data is openly available *via* dx.doi.org/10.5281/zenodo.5236823.

Author contributions

MFK conceived, supervised and led the project. MGA conducted most of the experimental work and analysed the data. MJM performed dye degradation experiments. FM conceived and supervised electrochemical measurements. MFK, MGA and FM wrote the manuscript.

Conflicts of interest

The authors declare no conflict of interest.

Acknowledgements

This work was supported by EPSRC through a DTA studentship to MGA (EP/R51312X/1), and a capital investment grant to MFK (EP/S017925/1). We thank Swansea University for providing start-up funds to MFK. We thank Prof. Alex Cowan and Dr Gaia Neri (University of Liverpool) for recording DR-UV spectra. We wish to thank Julian Kivell and Phil Hopkins in the Swansea University mechanical workshop for their assistance with the experimental setup. MFK is grateful to the Ernst Schering Foundation for support.

References

1 Y. Tachibana, L. Vayssieres and J. Durrant, *Nat. Photonics*, 2012, **6**, 511–518.
2 Q. Wang and K. Domen, *Chem. Rev.*, 2020, **120**, 919–985.
3 D. W. Wakerley and E. Reisner, *Energy Environ. Sci.*, 2015, **8**, 2283–2295.
4 P. M. Wood, *Biochem. J.*, 1988, **253**, 287–289.
5 M. T. Stiebritz and M. Reiher, *Chem. Sci.*, 2012, **3**, 1739–1751.
6 B. Mondal and A. Dey, *Chem. Commun.*, 2017, **53**, 7707–7715.
7 S. Chatterjee, K. Sengupta, S. Dey and A. Dey, *Inorg. Chem.*, 2013, **52**, 14168–14177.
8 N. Kaeffer, A. Morozan and V. Artero, *J. Phys. Chem. B*, 2015, **119**, 13707–13713.
9 F. Lakadamyali, M. Kato, N. M. Muresan and E. Reisner, *Angew. Chem., Int. Ed.*, 2012, **51**, 9381–9384.
10 Z.-H. Pan, Y.-W. Tao, Q.-F. He, Q.-Y. Wu, L.-P. Cheng, Z.-H. Wei, J.-H. Wu, J.-Q. Lin, D. Sun, Q.-C. Zhang, D. Tian and G.-G. Luo, *Chem. – Eur. J.*, 2018, **24**, 8275–8280.
11 T. Sakai, D. Mersch and E. Reisner, *Angew. Chem., Int. Ed.*, 2013, **52**, 12313–12316.
12 H. Li, D. Buesen, S. Dementin, C. Léger, V. Fourmond and N. Plumeré, *J. Am. Chem. Soc.*, 2019, **141**, 16734–16742.
13 A. Ruff, J. Szczesny, N. Marković, F. Conzuelo, S. Zacarias, I. A. C. Pereira, W. Lubitz and W. Schuhmann, *Nat. Commun.*, 2018, **9**, 3675.
14 C. Tapia, R. D. Milton, G. Pankratova, S. D. Minteer, H.-E. Åkerlund, D. Leech, A. L. De Lacey, M. Pita and L. Gorton, *ChemElectroChem*, 2017, **4**, 90–95.
15 S. Dey, A. Rana, D. Crouthers, B. Mondal, P. K. Das, M. Y. Darensbourg and A. Dey, *J. Am. Chem. Soc.*, 2014, **136**, 8847–8850.

16 Z. Li, B. Tian, W. Zhen, Y. Wu and G. Lu, *Appl. Catal., B*, 2017, **203**, 408–415.
17 K. Maeda, K. Teramura, D. Lu, N. Saito, Y. Inoue and K. Domen, *Angew. Chem., Int. Ed.*, 2006, **45**, 7806–7809.
18 A. T. Garcia-Esparza, T. Shinagawa, S. Ould-Chikh, M. Qureshi, X. Peng, N. Wei, D. H. Anjum, A. Clo, T.-C. Weng, D. Nordlund, D. Sokaras, J. Kubota, K. Domen and K. Takanabe, *Angew. Chem., Int. Ed.*, 2017, **56**, 5780–5784.
19 W. J. Jo, G. Katsoukis and H. Frei, *Adv. Funct. Mater.*, 2020, **30**, 1909262.
20 H. Li, U. Münchberg, A. A. Oughli, D. Buesen, W. Lubitz, E. Freier and N. Plumeré, *Nat. Commun.*, 2020, **11**, 920.
21 Y. Xu, J. P. Edwards, J. Zhong, C. P. O'Brien, C. M. Gabardo, C. McCallum, J. Li, C.-T. Dinh, E. H. Sargent and D. Sinton, *Energy Environ. Sci.*, 2020, **13**, 554–561.
22 X.-D. Lin, Y. Gu, X.-R. Shen, W.-W. Wang, Y.-H. Hong, Q.-H. Wu, Z.-Y. Zhou, D.-Y. Wu, J.-K. Chang, M.-S. Zheng, B.-W. Mao and Q.-F. Dong, *Energy Environ. Sci.*, 2021, **14**, 1439–1448.
23 E. L. Smith, A. P. Abbott and K. S. Ryder, *Chem. Rev.*, 2014, **114**, 11060–11082.
24 A. K. Halder and M. N. D. S. Cordeiro, *ACS Sustainable Chem. Eng.*, 2019, **7**, 10649–10660.
25 C. Vidal, J. García-Álvarez, A. Hernán-Gómez, A. R. Kennedy and E. Hevia, *Angew. Chem., Int. Ed.*, 2014, **53**, 5969–5973.
26 D. Arnodo, S. Ghinato, S. Nejrotti, M. Blangetti and C. Prandi, *Chem. Commun.*, 2020, **56**, 2391–2394.
27 J. A. McCune, M. F. Kuehnel, E. Reisner and O. A. Scherman, *Chem*, 2020, **6**, 1819–1830.
28 V. W.-H. Lau, I. Moudrakovski, T. Botari, S. Weinberger, M. B. Mesch, V. Duppel, J. Senker, V. Blum and B. V. Lotsch, *Nat. Commun.*, 2016, **7**, 12165.
29 W. Yang, R. Godin, H. Kasap, B. Moss, Y. Dong, S. A. J. Hillman, L. Steier, E. Reisner and J. R. Durrant, *J. Am. Chem. Soc.*, 2019, **141**, 11219–11229.
30 M. Heyrovský, *J. Chem. Soc., Chem. Commun.*, 1987, 1856–1857.
31 E. Reisner, D. J. Powell, C. Cavazza, J. C. Fontecilla-Camps and F. A. Armstrong, *J. Am. Chem. Soc.*, 2009, **131**, 18457–18466.
32 L. Ma, M. Liu, D. Jing and L. Guo, *J. Mater. Chem. A*, 2015, **3**, 5701–5707.
33 Z. Sun, H. Zheng, J. Li and P. Du, *Energy Environ. Sci.*, 2015, **8**, 2668–2676.
34 D. A. Reddy, H. Park, S. Hong, D. P. Kumar and T. K. Kim, *J. Mater. Chem. A*, 2017, **5**, 6981–6991.
35 S. Cao, Y. Chen, C.-J. Wang, X.-J. Lv and W.-F. Fu, *Chem. Commun.*, 2015, **51**, 8708–8711.
36 D. W. Wakerley, K. H. Ly, N. Kornienko, K. L. Orchard, M. F. Kuehnel and E. Reisner, *Chem. – Eur. J.*, 2018, **24**, 18385–18388.
37 L. Zhu, Q. Yue, D. Jiang, H. Chen, R. M. Irfan and P. Du, *Chin. J. Catal.*, 2018, **39**, 1753–1761.
38 L. Wang, R. Fernández-Terán, L. Zhang, D. L. A. Fernandes, L. Tian, H. Chen and H. Tian, *Angew. Chem., Int. Ed.*, 2016, **55**, 12306–12310.
39 L. Wang, H. Zhao, Y. Chen, R. Sun and B. Han, *Opt. Commun.*, 2016, **370**, 122–126.
40 T. R. Canterbury, S. M. Arachchige, K. J. Brewer and R. B. Moore, *Chem. Commun.*, 2016, **52**, 8663–8666.
41 L. Petermann, R. Staehle, M. Pfeifer, C. Reichardt, D. Sorsche, M. Wächtler, J. Popp, B. Dietzek and S. Rau, *Chem. – Eur. J.*, 2016, **22**, 8240–8253.
42 A. Call, Z. Codolà, F. Acuña-Parés and J. Lloret-Fillol, *Chem. – Eur. J.*, 2014, **20**, 6171–6183.
43 C. Vidal, J. García-Álvarez, A. Hernán-Gómez, A. R. Kennedy and E. Hevia, *Angew. Chem., Int. Ed.*, 2016, **55**, 16145–16148.
44 J. Schneider, D. Bahnemann, J. Ye, G. L. Puma and D. D. Dionysiou, *Photocatalysis: Fundamentals and Perspectives*, Royal Society of Chemistry, Cambridge, 2016.
45 A. Neudeck and L. Kress, *J. Electroanal. Chem.*, 1997, **437**, 141–156.
46 A. Szabo, D. K. Cope, D. E. Tallman, P. M. Kovach and R. M. Wightman, *J. Electroanal. Chem. Interfacial Electrochem.*, 1987, **217**, 417–423.
47 J. Weber, A. J. Wain and F. Marken, *Electroanalysis*, 2015, **27**, 1829–1835.
48 J. D. Wadhawan, P. J. Welford, H. B. McPeak, C. E. W. Hahn and R. G. Compton, *Sens. Actuators, B*, 2003, **88**, 40–52.
49 A. Schürmann, R. Haas, M. Murat, N. Kuritz, M. Balaish, Y. Ein-Eli, J. Janek, A. Natan and D. Schröder, *J. Electrochem. Soc.*, 2018, **165**, A3095–A3099.
50 K. Onda, E. Sada, T. Kobayashi, S. Kito and K. Ito, *J. Chem. Eng. Jpn.*, 1970, **3**, 18–24.
51 W. Lang and R. Zander, *Ind. Eng. Chem. Fundam.*, 1986, **25**, 775–782.
52 W. Xing, M. Yin, Q. Lv, Y. Hu, C. Liu and J. Zhang, in *Rotating Electrode Methods and Oxygen Reduction Electrocatalysts*, ed. W. Xing, G. Yin and J. Zhang, Elsevier, Amsterdam, 2014, pp. 1–31.
53 O. S. Hammond, D. T. Bowron and K. J. Edler, *Angew. Chem., Int. Ed.*, 2017, **56**, 9782–9785.
54 A. Y. M. Al-Murshedi, H. F. Alesary and R. Al-Hadrawi, *J. Phys.: Conf. Ser.*, 2019, **1294**, 052041.
55 W. Tong, M. Forster, F. Dionigi, S. Dresp, R. Sadeghi Erami, P. Strasser, A. J. Cowan and P. Farràs, *Nat. Energy*, 2020, **5**, 367–377.
56 S. L. Clegg and P. Brimblecombe, *Geochim. Cosmochim. Acta*, 1990, **54**, 3315–3328.
57 J. A. M. Abbas, PhD thesis, Swansea University, 1986.